

(μ^-, e^-) Conversion; A Symbiosis of Particle and Nuclear Physics

T. S. KOSMAS and J. D. VERGADOS

Theoretical Physics Division, University of Ioannina, GR 45110, Greece

Abstract

(μ^-, e^-) conversion is the experimentally most interesting lepton flavor violating process. From a theoretical point of view it is an interesting interplay of particle and nuclear physics. The effective transition operator, depending on the gauge model, is in general described in terms of a combination of four terms of transition operators (isoscalar and isovector, Fermi-like as well as axial vector-like). The experimentally most interesting ground state to ground state transition is adequately described in terms of the usual proton and neutron form factors. These were computed in both the shell model and RPA. Since it is of interest to know the portion of the strength exhausted by the coherent (ground state to ground state) transition, the total transition rate to all final states must also be computed. This was done i) in RPA by explicitly summing over all final states ii) in the context of the closure approximation (using shell model and RPA for constructing the initial state) and iii) in the context of nuclear matter mapped into nuclei via a local density approximation.

We found that, apart from small local oscillations, the conversion rate keeps increasing from light to heavy nuclear elements. We also find that the coherent mode is dominant (it exhausts more than 90% of the sum rule). Various gauge models are discussed. In general the predicted branching ratio is much smaller compared to the present experimental limit.

1 Introduction

All currently known experimental data are consistent with the standard model (SM) of weak and electromagnetic interactions. Within the framework of the SM, baryon and lepton quantum numbers are separately conserved. In fact one can associate an additive lepton flavor quantum number with each lepton generation which appears to be conserved. There are thus three such conserved quantum numbers L_e , L_μ and L_τ each one associated with the lepton generations (e^-, ν_e) , (μ^-, ν_μ) , (τ^-, ν_τ) , with their antiparticles having opposite lepton flavor. It is in fact these quantum numbers which distinguish between the three neutrino species if they are massless.

Most theorists, however, view the SM not as the ultimate theory of nature but as a successful low energy approximation. In possible extensions of the SM it is legitimate to ask whether lepton flavor conservation still holds. In fact in such gauge models (Grand Unified Theories, Supersymmetric Extensions of the SM, Superstring Inspired Models) such quantum numbers are associated with global (non local) symmetries and their conservation must be broken at some level.

Motivated in part by this belief the search for lepton flavor violation, which began almost half a century ago (Hincks and Pontecorvo, 1948 [1], Lagarigue and Peyrou, 1952 [2], Lokanathan and Steinberger, 1955 [3], see also Frankel, 1975 [4]) has been revived in recent years and is expected to continue in the near future. In the meantime the number of possible reactions for testing lepton flavor has been increased. The most prominent such reactions are

$$\mu \rightarrow e\gamma \tag{1}$$

$$\tau \rightarrow e\gamma \quad and \quad \tau \rightarrow \mu\gamma \tag{2}$$

$$\mu \rightarrow ee^+e^- \tag{3}$$

$$\tau \rightarrow ee^+e^-, \quad \tau \rightarrow \mu e^+e^- \tag{4}$$

$$\tau \rightarrow e\mu^+\mu^-, \quad \tau \rightarrow \mu\mu^+\mu^- \tag{5}$$

$$K_L \rightarrow \mu^\pm e^\mp, \quad K^+ \rightarrow \pi^+ \mu e \quad (6)$$

$$(\mu^+ e^-) \leftrightarrow (\mu^- e^+) \quad \text{muonium - antimuonium oscillations} \quad (7)$$

$$\mu^- + (A, Z) \rightarrow e^- + (A, Z) \quad (\text{muon - electron conversion}) \quad (8)$$

Finally, one could have both lepton and lepton flavor violating processes like

$$(A, Z) \rightarrow (A, Z \pm 2) + e^\mp e^\mp \quad (\beta\beta_{ov} - \text{decay}) \quad (9)$$

$$\mu^- + (A, Z) \rightarrow e^+ + (A, Z - 2) \quad (\text{muon - positron conversion}) \quad (10)$$

From an experimental point of view the most interesting reactions are (1), (3), (8), (9) and (10). None of the above processes has yet been seen. The best limits obtained are

$$R_{e\gamma} = \frac{\Gamma(\mu^+ \rightarrow e^+ \gamma)}{\Gamma(\mu^+ \rightarrow e^+ \nu_e \bar{\nu}_\mu)} < 4.9 \times 10^{-11} \quad (90\% \text{ CL}) \quad (11)$$

set by LAMPF (Bolton *et al.*, 1988 [5]),

$$R_{3e} = \frac{\Gamma(\mu^+ \rightarrow e^+ e^- e^+)}{\Gamma(\mu^+ \rightarrow \text{all})} < 1.0 \times 10^{-12} \quad (90\% \text{ CL}) \quad (12)$$

set by SINDRUM at PSI (Bellgardt *et al.*, 1988 [6]),

$$R_{e^- N} = \frac{\Gamma(\mu^- Ti \rightarrow e^- Ti)}{\Gamma(\mu^- \rightarrow \text{all})} < 4.6 \times 10^{-12} \quad (90\% \text{ CL}) \quad (13)$$

set by TRIUMF (Ahmad *et al.*, 1987 [7]) using a Time Projection Counter (TPC) and

$$R_{e^+ N} = \frac{\Gamma(\mu^- Ti \rightarrow e^+ Ca(gs))}{\Gamma(\mu^- \rightarrow \text{all})} < 4.4 \times 10^{-12} \quad (90\% \text{ CL}) \quad (14)$$

set by SINDRUM II (Badertscher *et al.*, 1991 [8]). For a Pb target the corresponding (μ^-, e^-) conversion limit is (Ahmad *et al.*, 1988 [7])

$$R_{e^-N} < 4.9 \times 10^{-10} \quad (90\% \text{ CL}) \quad (15)$$

From a theoretical physics point of view the problem of lepton flavor non-conservation is connected with the family mixing in the leptonic sector. Almost in all models the above process can proceed at the one loop level via the neutrino mixing. However, due to the GIM mechanism in the leptonic sector, the amplitude vanishes in the limit in which the neutrinos are massless. In some special cases the GIM mechanism may not be completely operative even if one considers the part of the amplitude which is independent of the neutrino mass (Langacker and London, 1988 [9], Valle, 1991 [10], Gonzalez-Garcia and Valle, 1992 [11]). Even then, however, the process is suppressed if the neutrinos are degenerate. It should be mentioned that processes (1)-(8) cannot distinguish between Dirac and Majorana neutrinos. Process (9) can proceed only if the neutrinos are Majorana particles.

In more elaborate models one may encounter additional mechanisms for lepton flavor violation. In Grand Unified Theories (GUT's) one may have additional Higgs scalars which can serve as intermediate particles at the one or two loop level leading to processes (1)-(8). In supersymmetric extensions of the standard model one may encounter as intermediate particles the superpartners of the above. Lepton flavor violation can also occur in composite models, e.g. technicolor [12]. In fact, such models have already been ruled out by the present experimental bounds (see eqs. (11)-(15)).

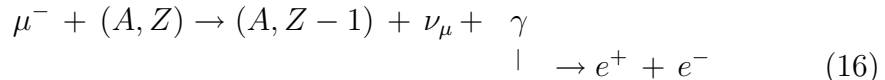
The observation of any of the processes (1)-(10) will definitely signal new physics beyond the standard model. It will severely restrict most models. It may take, however, even then much more experimental effort to unravel specific mechanisms responsible for lepton flavor violation or fix the parameters of the models. The question of lepton flavor non-conservation has been the subject of several review papers (Scheck, 1978 [13], Costa and Zwirner, 1986 [14], Engfer and Walter, 1986 [15], Vergados, 1986 [16], Bilenky and Petcov, 1987 [17], Melese, 1989 [18], Heusch, 1990 [19], Herczeg, 1992 [20], Schaaf, 1993 [21], Kosmas, Leontaris and Vergados, 1994 [22]). In the present review we will focus our attention on recent theoretical developments of the subject. We will pay little attention to the experimental situation, since we do not intend to duplicate the experimental review which recently appeared

(Schaaf, 1993 [21]). Furthermore, the reader can find an interesting account of the early experiments by Di Lella [23].

From a nuclear physics point of view the most interesting muon number violating process is the (μ^-, e^-) conversion in eq. (8). Its sister (μ^-, e^+) conversion in eq. (10) is much more complicated, since it involves two nucleons. Furthermore, lepton violation is more likely to be seen in neutrinoless double beta decay of eq. (9). In this report we will focus our attention on the (μ^-, e^-) conversion. We will concentrate mostly on the evaluation of nuclear matrix elements. As we have mentioned above, experimentally the most important transition is that to the ground state. It is, however, important to know which fraction of the total strength goes to the ground state. We will, therefore, also evaluate the total transition rate to all final states in various nuclear models.

The (μ^-, e^-) conversion, compared to its competitors $\mu \rightarrow e\gamma$, $\mu \rightarrow 3e$ etc., has some experimental advantages [22]:

1. The detection of only one particle is sufficient. No coincidence is needed.
 2. For electrons with the highest possible energy, i.e. $E_e \approx m_\mu c^2 - \epsilon_b$ with ϵ_b the muon binding energy, the reaction is almost background free. Indeed the reactions of induced background are:
 - i) Muon decay in orbit. There is a tiny tail in the region of interest which is proportional to $(E_{bg}^{max} - E_e)^5$, i.e. very small (E_{bg}^{max} denotes the maximum energy of the background electrons). But in this region the shape is known and it can be subtracted out.
 - ii) Radiative muon capture. Indeed this can be a source of background since the photon can decay to e^+e^- pairs as



If the neutrino and the positron carry away zero kinetic energy, the background electron can be confused with interesting electron. We notice, however, that the maximum electron energy for process (16) is

$$E_{bq}^{max} = m_\mu c^2 - \epsilon_b - m_e c^2 - \Delta = E_e - \Delta - m_e c^2 \quad (17)$$

where Δ is the difference in the binding energy of the two nuclei involved in eq. (16). By a judicious choice of the target nucleus Δ can be quite large (e.g. $\Delta = 2.5\text{MeV}$ for ^{12}C). Thus, one has a background free region if one restricts oneself to the coherent mode (the final nucleus of eq. (8) is left in its ground state).

2 Mechanisms for lepton flavor violation

Obviously, in all models which allow $\mu \rightarrow e\gamma$ to proceed [9, 22], reactions of eqs. (8), (9) and (10) can also proceed via a virtual photon (see fig. 1). The dot in these figures indicates that the vertex is not elementary but very complicated. Such processes are called photonic. Muon-electron conversion can, of course, occur via mechanisms which do not involve the photon (non-photonic mechanisms). These are Z-exchange diagrams, i.e. the photon of fig. 1(b) is replaced by a Z-boson. In most models these diagrams are less important than the photonic ones. Another possibility is an effective 4-fermion contact interaction (box diagrams). We notice that here it is possible to have both protons and neutrons participating which may lead to a nuclear enhancement (see fig. 2).

The most popular scenario for (μ^-, e^-) conversion involves intermediate neutrinos, see fig. 3 for the photonic case and fig. 4 for the box- diagram case. In these diagrams the neutrinos which propagate are the mass eigenstates. The neutrinos involved in weak interactions, ν_e and ν_μ , are not stationary states but linear combinations of neutrino mass eigenstates given by $U_{\mu j}$ and U_{ej} . Both light ν_j and heavy N_j intermediate neutrinos can propagate. Since, however, the matrix U is unitary, the part of the amplitude which is independent of the neutrino mass vanishes (GIM mechanism). Thus, the leading contribution is proportional to $\Delta m_\nu^2/M_W^2$, for light neutrinos, or $\Delta m_N^2 M_W^2/m_N^4$, for heavy neutrinos [16]. This means that the process is suppressed for neutrinos with masses very different from the W-boson mass. This is discouraging, since all reasonable models do not yield neutrinos in the region of the W-mass.

Another possibility is to enlarge the Higgs sector. One can induce (μ^-, e^-) conversion in models with two Higgs isodoublets. The most dominant contribution, however, is expected to occur at the two loop level [22]. This calculation has only been done for the $\mu \rightarrow e\gamma$ reaction. Such calculations

show that it is possible to reasonably adjust the parameters of the model so that a branching ratio not far from the experimental limit can be obtained. We should note, of course, that for real photons one encounters only the electric dipole and magnetic dipole form factors (see next section). For (μ^-, e^-) conversion (virtual photons) one also needs the monopole form factors which have not been calculated. One expects, however, to be able to obtain large branching ratios when this is accomplished for fast $\mu \rightarrow e\gamma$ decay.

Other exotic scalars, like the singly charged S^+ , the doubly charged isosinglet S^{++} and isotriplet χ^{++} , can also lead to flavor violations [16]. Such enlargements are not, however, favored by recent theoretical models, especially those which are superstring inspired, and they are not going to be further discussed.

Another interesting possibility is the supersymmetric extension of the standard model. One now has additional particles which are the superpartners of the known particles. With those extra particles participating as intermediaries one can have a plethora of new diagrams [22, 24]. The most important for (μ^-, e^-) conversion are shown in fig. 5.

The mixing matrix V entering the vertices is

$$V = S_e^+ S_{\bar{e}} \quad (18)$$

where S_e is the unitary mixing matrix for the charged leptons and $S_{\bar{e}}$ is the corresponding one for the S-leptons (see ref. [22]). To leading order (tree level) the matrices S_e and $S_{\bar{e}}$ are the same, i.e. V is diagonal, and lepton flavor violation occurs. If, however, one goes beyond the tree level and takes into account renormalization effects, the matrix V is no longer diagonal so that one can have lepton flavor violation [22].

3 Expressions for the amplitude of (μ^-, e^-) conversion

The amplitude for the (μ^-, e^-) conversion can be cast in the form [22]

$$\mathcal{M} = \frac{4\pi\alpha}{q^2} J_\lambda^{(1)} j_{(1)}^\lambda + \frac{\zeta}{m_\mu^2} J_\lambda^{(2)} j_{(2)}^\lambda \quad (19)$$

where the first term is the photonic and the second the non-photonic contribution. q is the momentum transfer and ζ takes the form

$$\zeta = \begin{cases} \frac{G_F m_\mu^2}{\sqrt{2}}, & \text{W-boson mediated models} \\ m_{3/2}^2/m_{\tilde{a}}^2, & \text{Supersymmetric models} \end{cases} \quad (20)$$

$m_{3/2}$ is the gravitino mass and $m_{\tilde{a}}$ is the relevant s -quark (supersymmetric partner of quark).

The hadronic currents are

$$J_\lambda^{(1)} = \bar{N} \gamma_\lambda \frac{1 + \tau_3}{2} N, \quad (\text{photonic}) \quad (21)$$

$$J_\lambda^{(2)} = \bar{N} \gamma_\lambda \frac{1}{2} [(3 + \beta f_V \tau_3) + (f_V + f_A \beta \tau_3) \gamma_5] N, \quad (\text{non-photonic}) \quad (22)$$

($N = \text{Nucleon}$) while the leptonic currents are

$$j_{(1)}^\lambda = \bar{u}(p_1) (f_{M1} + \gamma_5 f_{E1}) i \sigma^{\lambda\nu} \frac{q_\nu}{m_\mu} + (f_{E0} + \gamma_5 f_{M0}) \gamma^\nu \left(g_{\lambda\nu} - \frac{q^\lambda q^\nu}{q^2} \right) \quad (23)$$

$$j_{(2)}^\lambda = \bar{u}(p_1) \gamma^\lambda \frac{1}{2} (\tilde{f}_V + \tilde{f}_A \gamma_5) u(p_\mu) \quad (24)$$

where $\beta = \beta_1/\beta_0$, is the ratio of the isovector to the isoscalar component of the hadronic current at the quark level. The form factors f_{M1} , f_{E1} , f_{E0} , f_{M0} , \tilde{f}_V and \tilde{f}_A as well as the parameter β depend on the assumed gauge model and the mechanism adopted (the isoscalar parameter β_0 is absorbed in the definition of the leptonic form factors). For purely left-handed theories the number of independent form factors is reduced in half since

$$f_{E0} = -f_{M0}, \quad f_{E1} = -f_{M1}, \quad \tilde{f}_A = -\tilde{f}_V \quad (25)$$

In some models involving the W -boson one has

$$\frac{f_{E0}}{q^2} = -\frac{f_{E1}}{m^2} \quad (26)$$

while in the supersymmetric models discussed above one finds

$$f_{E0} = -f_{M0} = -\frac{1}{2}\tilde{\eta}\alpha^2 g(x)\frac{m_\mu^2}{m_{3/2}^2} \quad (27)$$

$$4\pi\alpha f_{E1} = -4\pi\alpha f_{M1} = -\frac{1}{2}\tilde{\eta}\alpha^2 f(x)\frac{m_\mu^2}{m_{3/2}^2} \quad (28)$$

$$\tilde{f}_V = -\tilde{f}_A = -\frac{\beta_0}{2}\tilde{\eta}\alpha^2 f_b(x)\frac{m_\mu^2}{m_{3/2}^2} \quad (29)$$

and

$$\beta_0 = \frac{4}{9} + \frac{1}{9}\frac{m_{\tilde{u}}^2}{m_d^2}, \quad \beta_1 = \frac{4}{9} - \frac{1}{9}\frac{m_{\tilde{u}}^2}{m_d^2} \quad (30)$$

The functions $g(x)$, $f(x)$, $f_b(x)$ depend on the quantity $\gamma = m_{\tilde{\gamma}}/m_{\tilde{a}}$. Since, however, this quantity is much smaller than unity, we get

$$f(x) \approx \frac{1}{12}, \quad g(x) \approx \frac{1}{18}, \quad f_b(x) \approx \frac{1}{8} \quad (31)$$

4 Effective nuclear transition operator and nuclear matrix elements

The first step in constructing the effective transition operator is to take the non-relativistic limit of the hadronic currents in eqs. (21), (22). This leads to the operators [22, 25, 26]

$$\Omega_0 = \tilde{g}_V \sum_{j=1}^A (3 + f_V \beta \tau_{3j}) e^{-i\mathbf{q} \cdot \mathbf{r}_j}, \quad \Omega = -\tilde{g}_A \sum_{j=1}^A (\xi + \beta \tau_{3j}) \frac{\sigma_j}{\sqrt{3}} e^{-i\mathbf{q} \cdot \mathbf{r}_j} \quad (32)$$

with $\xi = f_V/f_A$ and

$$\tilde{g}_V = \frac{1}{6}, \quad \tilde{g}_A = 0, \quad f_V = 1, \quad \beta = 3 \quad (\text{photonic case}) \quad (33)$$

$$\tilde{g}_V = \tilde{g}_A = \frac{1}{2}, \quad f_V = 1, \quad f_A = 1.24 \quad (\text{non-photonic case}) \quad (34)$$

For neutrino mediated processes

$$\beta_0 = \begin{cases} 30 \\ 1 \end{cases}, \quad \beta_1 = \begin{cases} 25 \\ 5/6 \end{cases} \quad \begin{array}{l} \text{light neutrinos} \\ \text{heavy neutrinos} \end{array} \quad (35)$$

i.e. $\beta = 5/6 \approx 0.8$ in both cases. For the supersymmetric model discussed above

$$\beta_0 \approx 5/9, \quad \beta_1 = \frac{1}{3}, \quad \text{i.e. } \beta = 0.6 \quad (36)$$

The factor $1/\sqrt{3}$ in Ω was introduced for convenience. Thus one has

$$|ME|^2 = f_V^2 |< f | \Omega_0 | i, \mu >|^2 + 3f_A^2 |< f | \Omega | i, \mu >|^2 \quad (37)$$

The second step is to factor out the muon 1s wave function [27, 28] i.e.

$$|< f | \Omega \Phi_\mu(\mathbf{r}) | i >|^2 \approx < \Phi_{1s}^2 > |< f | \Omega | i >|^2 \quad (38)$$

where

$$< \Phi_{1s}^2 > \equiv \frac{\int d^3r |\Phi_\mu(\mathbf{r})|^2 \rho(\mathbf{r})}{\int d^3r \rho(\mathbf{r})} \quad (39)$$

with $\Phi_\mu(\mathbf{r})$ the muon wave function and $\rho(\mathbf{r})$ the nuclear density. The above approximation was recently found to underestimate the width in heavy nuclei by as much as 40% (see below sect. 5). However, it is still a good approximation for the branching ratio R_{e-N} of eq. (13), since it affects both the numerator and the denominator by the same way.

With the above operators one can easily proceed with the evaluation of the relevant nuclear matrix elements. We distinguish the following two cases.

4.1 The coherent (μ^-, e^-) conversion matrix elements

For $0^+ \rightarrow 0^+$ transitions only the operator Ω_0 in eq. (37) contributes. One finds [22]

$$< i | \Omega_0 | i > = \tilde{g}_V (3 + f_V \beta) F(q^2) \quad (40)$$

where

$$F(q^2) = F_Z(q^2) + \frac{3 - f_V \beta}{3 + f_V \beta} F_N(q^2) \quad (41)$$

$$F_Z(q^2) = \frac{1}{Z} \int d^3r \rho_p(\mathbf{r}) e^{-i\mathbf{q}\cdot\mathbf{r}}, \quad F_N(q^2) = \frac{1}{N} \int d^3r \rho_n(\mathbf{r}) e^{-i\mathbf{q}\cdot\mathbf{r}} \quad (42)$$

F_Z and F_N are the proton, neutron nuclear form factors with $\rho_p(\mathbf{r})$, $\rho_n(\mathbf{r})$ the corresponding densities normalized to Z and N, respectively.

Then, the branching ratio R_{e^-N} takes the form

$$R_{e^-N} = \frac{1}{(G_F m_\mu^2)^2} \left\{ \left| \frac{m_\mu^2}{q^2} f_{M1} + f_{E0} + \frac{1}{2} \kappa \tilde{f}_V \right|^2 + \left| \frac{m_\mu^2}{q^2} f_{E1} + f_{M0} + \frac{1}{2} \kappa \tilde{f}_A \right|^2 \right\} \gamma_{ph} \quad (43)$$

where κ and γ_{ph} carry all the the dependence on the nuclear physics, i.e.

$$\gamma_{ph} = \frac{Z |F_Z(q^2)|^2}{G^2 f_{PR}(A, Z)} \quad (44)$$

and

$$\kappa = \left(1 + \frac{N}{Z} \frac{3 - \beta}{3 + \beta} \frac{F_N(q^2)^2}{F_Z(q^2)^2} \right) \zeta \quad (45)$$

In eq. (44) G^2 is a combination of the coupling constants entering the ordinary muon capture ($G^2 \approx 6$) and f_{PR} is the well known Primakoff function [27, 28] which adequately describes the ordinary muon capture throughout the periodic table. It is approximately given by [28]

$$f_{PR} \approx 1.6 \frac{Z}{A} - 0.62 \quad (46)$$

It is sometimes convenient to factor out the nuclear dependence from the dependence on the rest parameters of the theory [29], i.e. we write

$$R_{e^-N} = \rho \gamma \quad (47)$$

where the quantity ρ is independent on nuclear physics. The quantity γ takes the form

$$\gamma = \frac{|\mathcal{M}E|^2}{G^2 Z f_{PR}(A, Z)} \quad (48)$$

In the case of the supersymmetric model discussed above γ takes the form

$$\gamma = \left(\frac{1}{3} + \frac{3\kappa}{4} \right)^2 \gamma_{ph.} \quad (49)$$

At this point it is of interest to compare the branching ratio of (μ^-, e^-) conversion to that of the $\mu \rightarrow e\gamma$ decay. One finds

$$\frac{R_{e^-N}}{R_{e\gamma}} \approx \frac{\alpha}{6\pi} \left(\frac{1}{3} + \frac{3\kappa}{4} \right)^2 \gamma_{ph} \quad (50)$$

4.2 Total (μ^-, e^-) conversion matrix elements

As it was mentioned in the introduction, only the coherent rate is of experimental interest. It is, however, important to know what portion of the sum rule is exhausted by the coherent mode. We thus have to evaluate the total matrix element

$$M_{tot}^2 = f_V^2 \sum_f \left(\frac{q_f}{m_\mu} \right)^2 | \langle f | \Omega_0 | i \rangle |^2 + 3f_A^2 \sum_f \left(\frac{q_f}{m_\mu} \right)^2 | \langle f | \Omega | i \rangle |^2 \quad (51)$$

where

$$q_f = m_\mu - \epsilon_b - (E_f - E_{gs}) \quad (52)$$

E_f, E_{gs} are the energies of the final and ground state of the nucleus. This evaluation clearly can be done in a model in which the final states can be explicitly constructed. This is a formidable task, however, and only in simple models can easily be done (e.g. RPA [26, 30]).

The other alternative is to use some approximation scheme. The first is the so-called "closure approximation" [25, 31]. In this approximation one first replaces the momentum q_f by a suitable average, i.e. $q_f \rightarrow k = \langle q_f \rangle$. Thus [22],

$$\Omega_0(\mathbf{q}_f) \approx \sum_j \omega_0(j) e^{-i\mathbf{k} \cdot \mathbf{r}_j} \equiv \Omega_0(\mathbf{k}) \quad (53)$$

$$\Omega(\mathbf{q}_f) \approx \sum_j \omega(j) e^{-i\mathbf{k} \cdot \mathbf{r}_j} \equiv \Omega(\mathbf{k}) \quad (54)$$

where

$$\omega_0(j) = 3 + f_V \tau_{3j}, \quad \omega(j) = (\xi + \beta \tau_{3j}) \sigma / \sqrt{3} \quad (55)$$

Then, we write

$$\begin{aligned} S_A &= \sum_f \left(\frac{q_f}{m_\mu} \right)^2 | \langle f | \Omega(\mathbf{q}_f) | i \rangle |^2 \\ &\approx \frac{k^2}{m_\mu^2} \sum_f \langle i | \Omega^+(k) | f \rangle \cdot \langle f | \Omega(k) | i \rangle \end{aligned} \quad (56)$$

or using closure over the final states we get

$$S_A = \frac{k^2}{m_\mu^2} \langle i | \Omega^+(k) \cdot \Omega(k) | i \rangle = \frac{k^2}{m_\mu^2} \left\{ \langle i | \Omega_{1b} | i \rangle + \langle i | \Omega_{2b} | i \rangle \right\} \quad (57)$$

where

$$\Omega_{1b} = \sum_j \omega^+(j) \cdot \omega(j) \quad (58)$$

$$\Omega_{2b} = \sum_{i \neq j} \omega^+(i) \cdot \omega(j) e^{-i\mathbf{k} \cdot (\mathbf{r}_i - \mathbf{r}_j)} \quad (59)$$

The computation of S_V is analogous with

$$\Omega_{1b} = \sum_j \omega_0^+(j) \omega_0(j) \quad (60)$$

$$\Omega_{2b} = \sum_{i \neq j} \omega_0^+(i) \omega_0(j) e^{-i\mathbf{k} \cdot (\mathbf{r}_i - \mathbf{r}_j)} \quad (61)$$

We thus find

$$M_{tot}^2 = f_V^2 S_V + 3f_A^2 S_A \quad (62)$$

The real question is what is the appropriate value of k ? In earlier calculations [25, 31] an average excitation energy $\bar{E} = 20\text{MeV}$ was used which was derived from the ordinary muon capture phenomenology. It was recently realized, however, that the correct excitation energy must be appreciably smaller [26] due to the presence in (μ^-, e^-) conversion of the coherent mode with $E_f = 0$. This channel is absent in muon capture. It seems reasonable, therefore, to use an average energy defined by

$$\bar{E} = \frac{\sum_f (E_f - E_{gs}) \left(\frac{|\mathbf{q}_f|}{m_\mu}\right)^2 |\langle f | \Omega | gs \rangle|^2}{\sum_f \left(\frac{|\mathbf{q}_f|}{m_\mu}\right)^2 |\langle f | \Omega | gs \rangle|^2} \quad (63)$$

This definition cannot in practice be used since presupposes knowledge of the final states, which we like to avoid. It can, therefore, be estimated in a simple model like RPA (see next section). In the context of RPA we can also estimate easily the effect of the $gs \rightarrow gs$ correlations by using the Thouless theorem and defining a correlated vacuum in terms of the uncorrelated one (see ref. [22, 26]). This shows that both the coherent as well as the total (μ^-, e^-) conversion matrix elements are a rescaling of the uncorrelated ones and that the ground state correlations strongly reduce all matrix elements (see sect. 5).

Another method for calculating the (μ^-, e^-) conversion widths has recently been proposed by the Valencia group [32, 33, 34]. This method employs nuclear matter mapped into nuclei via a local density approximation (L.D.A.) utilizing the relativistic Lindhard function. It has been proved that this method reproduces very well the ordinary muon capture data. In this process only the incoherent channels are open. The method, however, has been also applied to the incoherent part of (μ^-, e^-) conversion [35]. The Lindhard function was computed taking into account particle-hole excitations of p-n type in a local Fermi sea without invoking the approximation of eq. (38). The coherent mode is evaluated independently by using a local density approximation in eq. (37).

5 Results and discussion

As we have mentioned in the introduction, in the present report we focus on the nuclear dependence of (μ^-, e^-) conversion rates. In this section we

present and discuss the nuclear matrix elements for both the ground state to ground state transition (coherent mode) and the sum over all final states (total rate) obtained in the context of the three methods discussed above, i.e. (i) shell model, (ii) quasi-particle RPA and (iii) nuclear matter mapped into nuclei.

5.1 Coherent (μ^-, e^-) conversion

For the coherent mode one essentially needs only calculate the proton and neutron nuclear form factors. In table 1 the results for the $0^+ \rightarrow 0^+$ transition matrix elements obtained in the framework of the shell model and quasi-particle RPA are shown. They describe the mechanism for the photonic diagrams ($\beta = 3$) and non-photonic ones ($\beta = 5/6$) discussed in sect. 2. We see that the two methods give about the same results. In both methods we have followed the conventional approach and ignored the muon binding energy (see table 1 results labeled shell model and QRPA(i)). To check the validity of this approximation the calculation was repeated in the context of RPA (see table 1 results labeled QRPA(ii)) by explicitly calculating the binding energy ϵ_b . For heavy nuclei it was found that the consideration of ϵ_b gives about 40% larger results. This is expected, since in this case the momentum transfer at which the form factors are calculated is smaller.

We mention that similar results have also been found by using ϵ_b with the method of nuclear matter mapped into nuclei [35]. These results are shown in table 2. With the latter method the accuracy of using the approximation of eq. (38) was also tested by doing exact calculation of the muon-nucleus overlap which is possible in the context of the nuclear matter mapped into nuclei method [35]. We see that the exact calculations for the absolute rates (case II of table 2) differ appreciably from those of the approximation of eq. (38) (case I of table 2). We should mention, however, that we expect this approximation to be much better in the branching ratio provided that the total (μ^-, ν_μ) rate is calculated in the same way. One then can use the Primakoff's function (see eqs. (44) and (46)) which was derived under this approximation.

The effect of the ground state to ground state correlations was estimated in the context of RPA as was discussed in sect. 4.2. The results obtained for ^{48}Ti nucleus are shown in tables 3 and 4. We see that these correlations reduce both the coherent and total matrix elements by about 30% which is

in agreement with other similar results [36, 37].

5.2 Incoherent (μ^-, e^-) conversion

The incoherent (μ^-, e^-) conversion involves the matrix elements of all the excited states of the participating nucleus. These have been calculated with two methods: (i) by explicitly constructing the final states in the context of the quasi-particle RPA [26] (see tables 3 and 4 results labeled QRPA(explicit)) and (ii) by summing over a continuum of excited states in a local Fermi sea in the framework of the nuclear matter mapped into nuclei method [35] (see results labeled L.D.A. in table 3).

The total rates have also been obtained by assuming closure approximation and employing a mean excitation energy of the studied nucleus as was discussed in sect. 4.2. The results obtained this way both in the context of shell model [25] and RPA sum rules [26] are shown in tables 3 and 4 for various mean excitation energies \bar{E} (see sect. 4.2 for details). For RPA the mean excitation energy used was found by firstly calculating one by one the excited states included in eq. (51). Since such a calculation in the context of the shell model is very tedious, the value of \bar{E} used in shell model sum rules was chosen in analogy to that of the muon capture reaction. The big difference appeared between the two values is justified because, in the (μ^-, e^-) conversion the dominant $gs \rightarrow gs$ transition (not existing in the muon capture) contributes only in the non energy weighted sum rule of eq. (63). The above large mean excitation energy used in shell model sum rules overestimated the incoherent matrix elements (especially in the region of heavy nuclei), since they depend strongly on \bar{E} .

As we have stressed above, among all the open channels for (μ^-, e^-) conversion the transition to the ground state is of experimental interest. A useful quantity is the ratio of the coherent rate divided by the total (μ^-, e^-) rate, i.e.

$$\eta = \frac{|\text{ME}|_{coh}^2}{|\text{ME}|_{tot}^2} \quad (64)$$

By dividing the results obtained for the coherent mode ($M_{gs \rightarrow gs}^2$) and the total (μ^-, e^-) matrix elements (M_{tot}^2), either they are given directly from a sum rule or by adding independent coherent and incoherent results, we found

that the coherent channel dominates (see tables 3 and 4) and that throughout the periodic table $\eta \geq 90\%$ (see ref. [30] and [35]).

6 Summary and conclusions

In this report we have investigated the $(A, Z)(\mu^-, e^-)(A, Z)^*$ reaction emphasizing its dependence on nuclear physics. Using reasonable assumptions it was possible to factor out the nuclear dependence. The nuclear matrix elements of great interest were those entering the ground state to ground state transition. These were described in terms of proton and neutron form factors. Shell model calculations give similar results with RPA [26]. The predicted proton form factors agree with those extracted from electron scattering. As expected [36, 37] ground state correlations reduce the rates by as much as 30%. The predicted proton form factors agree with those extracted from electron scattering.

The total matrix element was also computed. First, by explicit calculations involving all the final states in the context of RPA. Second, by employing a sum rule with a suitable mean excitation energy $\bar{E} \approx 2\text{MeV}$, i.e. much smaller than previously expected [25]. This was done both in shell model and RPA. Again the ground state correlations tend to decrease the predicted rates. For the calculation of the total rate we also used a new method which employs nuclear matter mapped into nuclei via a local density approximation. Needless to say that, though all three methods basically agree with each other, the accuracy of such calculations is not as good as those for the coherent process. It is, however, pretty certain to expect that throughout the periodic table the coherent mode dominates, i.e. $\eta \geq 90\%$. This, as we have mentioned in the introduction, is experimentally very important.

Returning to the coherent production we find that there is some dependence on nuclear physics. In fact we find that

$$1.67 \leq \kappa \leq 1.89 \quad (65)$$

(see eq. (45)) which is a small effect. The variation in γ_{ph} is, however, much more pronounced.

$$1.6 \leq \gamma_{ph} \leq 26 \quad (66)$$

The (μ^-, e^-) conversion rate does not show a maximum around $A \approx 60$, as it was previously believed [38], but keeps increasing all the way up to the heaviest elements [35].

The nuclear dependence on (A, Z) is not strong enough to overcome the extra power of α in eq. (50). We find

$$1.5 \times 10^{-3} \leq \frac{R_{e^-N}}{R_{e\gamma}} \leq 3 \times 10^{-2} \quad (67)$$

(the largest refers to ^{132}Sn and the lowest to ^{12}C).

Finally, it is not encouraging that the predicted branching ratios for the muon number violating processes are much smaller than experiment. In the supersymmetric model described above we find

$$1.2 \times 10^{-18} \leq R_{e^-N} \leq 2.4 \times 10^{-16} \quad (68)$$

We must stress, however, that this should not discourage the experimentalists, since we do not as yet have a complete theory to adequately describe such processes.

References

- [1] E. P. Hincks and B. Pontecorvo, Phys. Rev. **73** (1948) 257
- [2] A. Lagarigue and C. R. Peyrou, Acad. Sc. (Paris) **234** (1952) 1873
- [3] S. Lokanathan and J. Steinberger, Phys. Rev. **98** (1955) 240
- [4] S. Frankel, Rare and ultrarare Muon decay, in Muon Physics II, Weak interactions, ed. by V. W. Hughes and C. S. Wu, Academic Press, New York 1975, p. 83.
- [5] R. D. Bolton *et al.*, Phys. Rev. **D 38** (1988) 2077
- [6] U. Bellgardt *et al.*, (SINDRUM Collaboration), Nucl. Phys. **B 299** (1988) 1
- [7] S. Ahmad *et al.*, Phys. Rev. Lett. **59** (1987) 970; Phys. Rev. **D 38** (1988) 2102

- [8] A. Badertscher *et al.*, (SINDRUM Collaboration), J. of Phys. **G 17** (1991) S47
- [9] P. Langacker and D. London, Phys. Rev. **D 38** (1988) 907
- [10] J. W. F. Valle, Prog. Part. Nucl. Phys. **26** (1991) 91
- [11] M. C. Gonzalez-Garcia and J. W. F. Valle, Mod. Phys. Lett. **A 7** (1992) 477.
- [12] S. Dimopoulos, S. Raby and G. L. Kane, Nucl. Phys. **B 182** (1981) 77; S. Dimopoulos and J. Ellis, Nucl. Phys. **B 182** (1981) 505
- [13] F. Scheck, Phys. Rep. **44** (1978) 187
- [14] G. Costa and F. Zwirner, Riv. Nuovo Cim. **9, 3** (1986) 1
- [15] R. Engfer and H. K. Walter, Ann. Rev. Nucl. Part. Sci. **36** (1986) 327.
- [16] J. D. Vergados, Phys. Rep. **133** (1986) 1.
- [17] S. M. Bilenky and S. T. Petcov, Rev. Mod. Phys. **59** (1987) 671
- [18] P.L. Melese, Comments on Nucl. Part. Phys. **19** (1989) 117.
- [19] C.A. Heusch, Nucl. Phys. (Proc. Suppl.) **B 13** (1990) 612.
- [20] P. Herczeg, Rare decays, Proc. 3rd Int. Symp. on weak and EM int. in Nuclei (Wein 1992), Dubna, Russia, 1992, ed. Ts. D. Vylov, World Scientific, Singapore 1993, p. 262
- [21] A. van der Schaaf, Prog. Part. Nucl. Phys. **31** (1993) 1.
- [22] T. S. Kosmas, G. K. Leontaris and J. D. Vergados, Prog. Part. Nucl. Phys. **33** (1994), 457.
- [23] L. Di Lella, Phys. Rep. **225** (1993) 45
- [24] T. S. Kosmas, G. K. Leontaris and J. D. Vergados, Phys. Lett. **B 219** (1989) 419
- [25] T.S. Kosmas and J. D. Vergados, Nucl. Phys. **A 510** (1990) 641.

- [26] T. S. Kosmas, J. D. Vergados, O. Civitarese and A. Faessler, Nucl. Phys. **A 570** (1994) 637.
- [27] H. Primakoff, Rev. Mod. Phys. **31** (1959) 802
- [28] B. Goulard and H. Primakoff, Phys. Rev. **C 10** (1974) 2034
- [29] T. S. Kosmas and J.D. Vergados, Phys. Lett. **B 215** (1988) 460.
- [30] T. S. Kosmas, A. Faessler, F. Simkovic and J. D. Vergados, in preparation and Proc. 5th Hellenic Symp. on Nucl. Phys., Ioannina 1-2 Oct, 1993, ed. by X. Aslanoglou, T.S. Kosmas and G. Pantis, (University Press, 1994).
- [31] T. S. Kosmas and J. D. Vergados, Phys. Lett. **B 217** (1989) 19.
- [32] H. C. Chiang, E. Oset and P. Fernandez de Cordoba, Nucl. Phys. **A 510** (1990) 591.
- [33] H. C. Chiang, E. Oset, R. C. Carrasco, J. Nieves and J. Navarro, Nucl. Phys. **A 510** (1990) 573.
- [34] C. Garcia-Recio, J. Nieves and E. Oset, Nucl. Phys. **A 547** (1992) 473.
- [35] H. C. Chiang, E. Oset, T. S. Kosmas, A. Faessler and J. D. Vergados, Nucl. Phys. **A 559** (1993) 526
- [36] P. J. Ellis, Nucl. Phys. **A 467** (1987) 173
- [37] J. A. McNeil, C. E. Price and J. R. Shepard, Phys. Rev. **C 42** (1990) 2442
- [38] S. Weinberg and G. Feinberg, Phys. Rev. **Lett. 3** (1959) 111

Table 1: Coherent (μ^-, e^-) conversion matrix elements $M_{gs \rightarrow gs}^2$ calculated in the context of shell model and quasi-particle RPA (see text).

Nucleus (A, Z)	Photonic Mechanism ($\beta = 3$)			Non-Photonic Mechanism ($\beta = 5/6$)		
	Shell Model	QRPA (i)	QRPA (ii)	Shell Model	QRPA (i)	QRPA (ii)
$^{48}_{22}Ti_{26}$	142.7	135.2	139.6	374.3	363.2	375.2
$^{60}_{28}Ni_{32}$	187.5	187.8	198.7	499.6	498.2	527.4
$^{72}_{32}Ge_{40}$	212.9	212.7	227.8	595.8	596.2	639.5
$^{112}_{48}Cd_{64}$	274.2	280.0	346.7	769.4	785.8	983.3
$^{162}_{70}Yb_{92}$	313.6	311.0	484.3	796.0	840.3	1412.1
$^{208}_{82}Pb_{126}$	240.2	287.5	582.9	631.4	767.5	1674.9

Figure Captions

Fig. 1

Photonic diagrams for the elementary process $\mu \rightarrow e\gamma$, fig. 1(a), and the induced processes (μ^-, e^-) conversion, fig. 1(b), $\mu \rightarrow e^+e^-$, fig. 1(c) and muonium-antimuonium oscillations, fig. 1(d). \bullet is a complicated vertex.

Fig. 2

Box-diagrams of (μ^-, e^-) conversion in an effective 4-fermion contact interaction. Both protons and neutrons participate.

Fig. 3

Table 2: Coherent widths (in arbitrary units) for the photonic and non-photonic mechanisms obtained with the exact muon wave function (column labeled I) and with the approximation of eq. (38) (column labeled II).

Nucleus		non-photonic mechanism ($\beta = 5/6$)	photonic mechanism ($\beta = 3$)		
A	Z	I	II	I	II
12	6	$0.52 \cdot 10^{-4}$	$0.51 \cdot 10^{-4}$	$0.21 \cdot 10^{-4}$	$0.21 \cdot 10^{-4}$
24	12	$0.91 \cdot 10^{-3}$	$0.90 \cdot 10^{-3}$	$0.38 \cdot 10^{-3}$	$0.37 \cdot 10^{-3}$
27	13	$0.14 \cdot 10^{-2}$	$0.14 \cdot 10^{-2}$	$0.56 \cdot 10^{-3}$	$0.55 \cdot 10^{-3}$
32	16	$0.29 \cdot 10^{-2}$	$0.28 \cdot 10^{-2}$	$0.12 \cdot 10^{-2}$	$0.12 \cdot 10^{-2}$
40	20	$0.64 \cdot 10^{-2}$	$0.62 \cdot 10^{-2}$	$0.27 \cdot 10^{-2}$	$0.26 \cdot 10^{-2}$
44	20	$0.72 \cdot 10^{-2}$	$0.69 \cdot 10^{-2}$	$0.26 \cdot 10^{-2}$	$0.25 \cdot 10^{-2}$
48	22	$0.94 \cdot 10^{-2}$	$0.91 \cdot 10^{-2}$	$0.35 \cdot 10^{-2}$	$0.34 \cdot 10^{-2}$
63	29	$0.21 \cdot 10^{-1}$	$0.19 \cdot 10^{-1}$	$0.78 \cdot 10^{-2}$	$0.72 \cdot 10^{-2}$
90	40	$0.47 \cdot 10^{-1}$	$0.42 \cdot 10^{-1}$	$0.17 \cdot 10^{-1}$	$0.16 \cdot 10^{-1}$
112	48	$0.62 \cdot 10^{-1}$	$0.54 \cdot 10^{-1}$	$0.22 \cdot 10^{-1}$	$0.19 \cdot 10^{-1}$
208	82	$0.13 \cdot 10^0$	$0.89 \cdot 10^{-1}$	$0.41 \cdot 10^{-1}$	$0.29 \cdot 10^{-1}$
238	92	$0.12 \cdot 10^0$	$0.73 \cdot 10^{-1}$	$0.35 \cdot 10^{-1}$	$0.22 \cdot 10^{-1}$

Table 3: Total and coherent (μ^-, e^-) matrix elements for ^{48}Ti (non-photonic mechanism, $\beta = 5/6$). The ratio η of eq. (64) is also shown.

Method	$M_{gs \rightarrow gs}^2$	\bar{E}	M_{tot}^2	η (%)
<i>L.D.A.</i>	375.7		410.5	91.5
<i>Shell Model</i> (sum – rule)	374.3	20.0	468.0	80.0
<i>QRPA</i> (<i>explicit</i>)	363.0	-	386.4	93.9
<i>QRPA</i> (sum – rule)	363.0	0.5	366.2	99.1
<i>QRPA</i> (sum – rule)	363.0	5.0	376.5	96.4
<i>QRPA</i> (sum – rule)	363.0	20.0	382.8	94.8
<i>QRPA + Corr</i> (sum – rule)	236.2	0.5	238.6	99.0
<i>QRPA + Corr</i> (sum – rule)	236.2	5.0	245.4	96.3
<i>QRPA + Corr</i> (sum – rule)	236.2	20.0	249.5	94.7

Table 4: Total and coherent (μ^-, e^-) matrix elements for the photonic mechanism ($\beta = 3$). See caption of table 3.

Method	$M_{gs \rightarrow gs}^2$	\bar{E}	M_{tot}^2	η (%)
<i>Shell Model</i> (sum – rule)	144.6	20.0	188.8	67.2
<i>QRPA</i> (<i>explicit</i>)	135.0	-	146.2	92.3
<i>QRPA</i> (sum – rule)	135.0	1.7	138.3	97.6
<i>QRPA</i> (sum – rule)	135.0	5.0	140.6	96.0
<i>QRPA</i> (sum – rule)	135.0	20.0	141.7	95.3
<i>QRPA + Corr</i> (sum – rule)	87.8	1.7	90.4	97.1
<i>QRPA + Corr</i> (sum – rule)	87.8	5.0	91.8	95.6
<i>QRPA + Corr</i> (sum – rule)	87.8	20.0	92.6	94.8

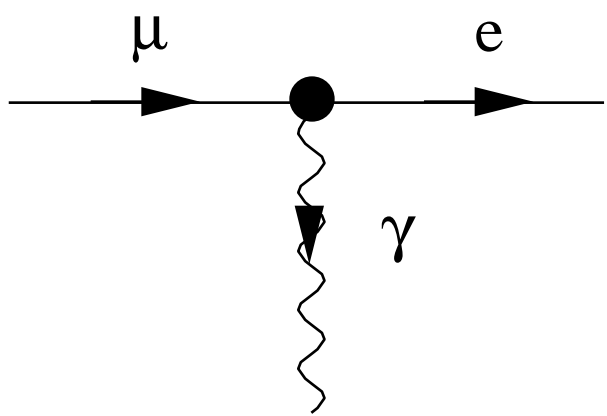
Photonic diagrams of (μ^-, e^-) conversion in a model with mixed intermediate neutrinos.

Fig. 4

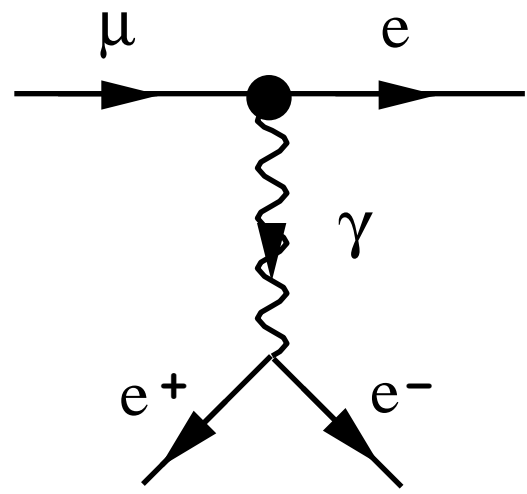
Box diagrams (for protons and neutrons) of (μ^-, e^-) conversion in a model with mixed intermediate neutrinos.

Fig. 5

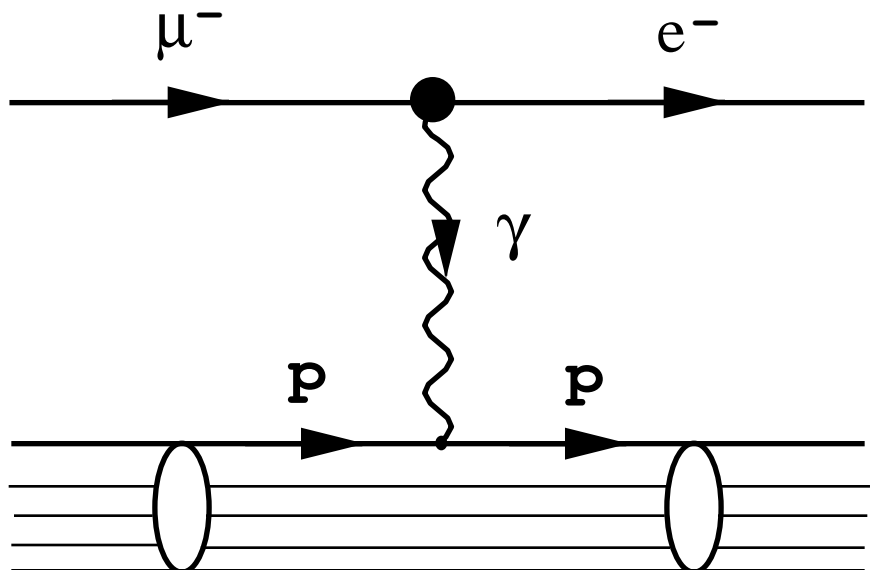
SUSY diagrams for (μ^-, e^-) conversion. Intermediate charged s-lepton mixing.



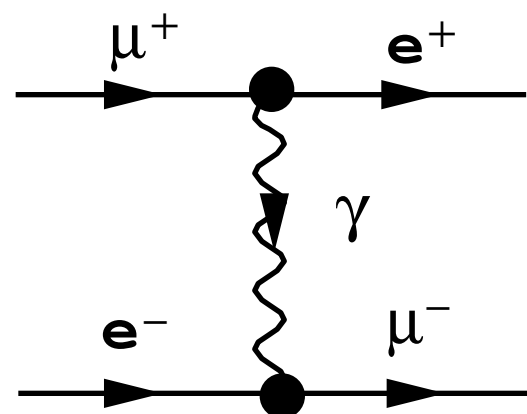
(a)



(c)



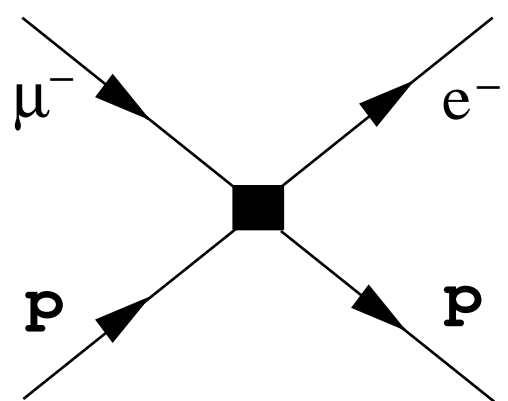
(b)



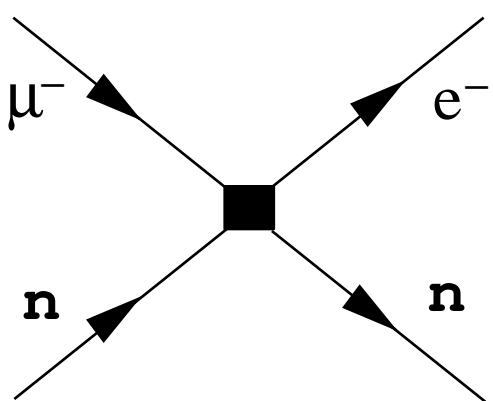
(d)

This figure "fig1-1.png" is available in "png" format from:

<http://arxiv.org/ps/nucl-th/9408011v1>

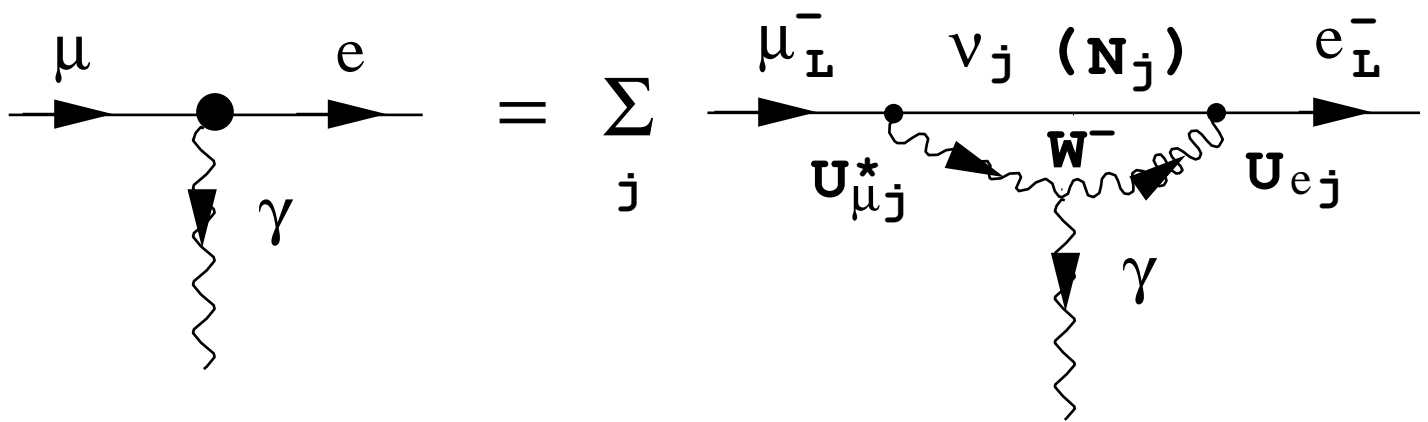


+



This figure "fig1-2.png" is available in "png" format from:

<http://arxiv.org/ps/nucl-th/9408011v1>



+ photon from charged leptons

